# Integrated Neuromorphic Information Processing with Electrically-injected Microring Spiking Neuron

**Jinlong Xiang, Yaotian Zhao, Xuhan Guo*, and Yikai Su**
*State Key Lab of Advanced Optical Communication Systems and Networks, Department of Electronic Engineering, Shanghai Jiao Tong University, Shanghai 200240, China*
*Author e-mail address: guoxuhan@sjtu.edu.cn*

**Abstract:** We experimentally demonstrate, for the first time, a CMOS-compatible electrically injected microring spiking neuron, capable of reproducibly emulating the typical neural dynamics including excitability threshold, temporal integration, refractory period, and spike inhibition. © 2024 The Author(s)

## 1. Introduction

In the past few years, the booming of artificial intelligence (AI) and machine learning has revolutionized almost every aspect of human life, from daily applications like voice recognition, and weather forecasting to scientific research like drug discovery, protein structure prediction, etc[1]. However, it becomes increasingly challenging for electronic processors to meet the exponential growth of computing demand of AI, owing to the fundamental bottlenecks of radiative physics, RC constant, and the typical bandwidth–distance–energy limits in electronic links. As a promising alternative, photonic technology offers fascinating advantages such as high parallelism, broad bandwidth, low crosstalk, and large integration for next-generation neuromorphic systems[2]. Compared to the continuous-value-based artificial neural network (ANN) and the convolutional neural network (CNN), the brain-inspired spiking neural network (SNN) offers a more biologically plausible way to realize neuromorphic computing due to its rich temporal information and the event-driven manner[3]. Photonic spiking neurons reported so far are most implemented with different types of lasers such as quantum dots, distributed feedback lasers, and vertical-cavity surface-emitting lasers (VCSELs), which underly similar excitability mechanisms with biological neurons shown in Fig. 1(a)[4]. Although typical neuron-like dynamics as well as simple pattern recognition tasks have already been experimentally demonstrated with either bulk discrete devices[5, 6] or integrated laser chips[7, 8], it still faces great difficulties in building integrated large-scale SNNs, considering the poor compatibility of III-V materials with the mutual complementary metal–oxide–semiconductor (CMOS) fabrication process.

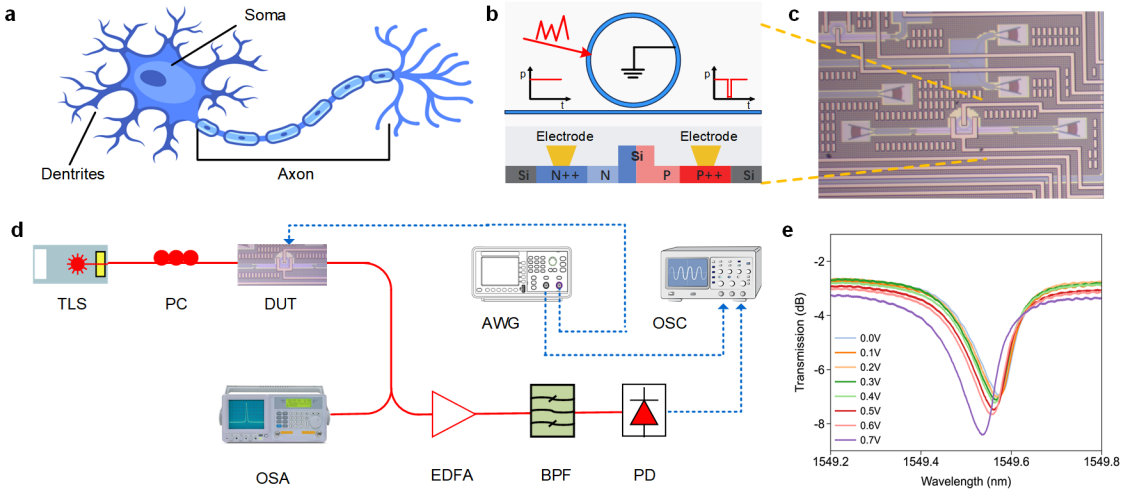


Fig. 1. (a) Illustration of a biological neuron, (b) working principle of the microring spiking neuron and cross-section view of the embedded p-n junction. (c) microscope image of the fabricated microring neuron. (d) experimental setup for both the characterization of the microring and investigation of its spiking dynamics. (e) transmission spectra under different bias voltages.

Recently, a novel all-optical spiking neuron has been proposed by utilizing the interplay of the fast free carrier dynamics and the slow thermal effect in a silicon microring[9]. Nevertheless, the simultaneous wavelength and power configuration of the pump and perturbation light can be very complicated when it's organized to build a SNN. Moreover, the slow thermal relaxation process sets an upper limit on its operation speed. Here, we experimentally

demonstrate, for the first time, a silicon microring with an embedded p-n junction can emulate a spiking neuron under proper electrical injection, exhibiting representative neuron-like functionalities including excitability threshold, temporal integration, refractory period, and spike inhibition. Besides, binary-to-spike information encoding is successfully verified at a speed of 250 MHz, comparable to that of laser-based spiking neurons[7, 8].

## 2. Results

As presented in Fig. 1(b), the microring is designed with an embedded p-n junction. When the pump light is appropriately configured to bias the microring near the excitable regime, electrical perturbation pulses can trigger the microring to emit 'negative' spiking responses. The microring neuron is fabricated with a commercial 180 nm CMOS process in CUMEC within a multi-project wafer (MPW). Fig. 1(c) is the microscope picture before packaging with wire bonding. The experimental setup is schematically illustrated in Fig 1(d), where optical fiber connections are shown in red and electrical connections are presented in blue. Figure 1(e) gives the measured non-normalized transmission spectra under different bias voltages. The microring has a resonance at 1549.575 nm with an extinction ratio of ~ 4.22 dB. The 3 dB bandwidth is about ~68 pm, corresponding to a quality factor (Q) of 22,800. As the bias voltage gradually increases, the concentration of free carriers in the waveguide becomes higher, thus leading to the blue shift of the microring resonance, owing to the free carrier dispersion (FCD) effect.

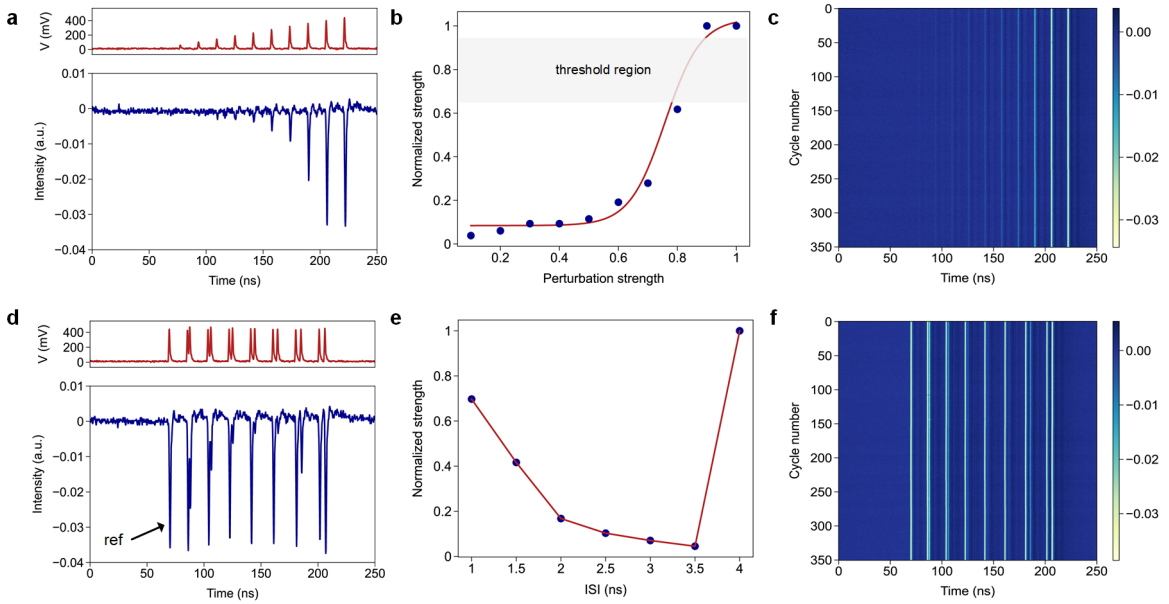


Fig. 2. Experimental demonstration of the excitability and refractory period dynamics. (a) Spike response of the microring to perturbation pulses of different power, (b) dependence of the normalized output on the perturbation strength, (c) temporal map that plots the continuous time traces of (a) as cycling patterns, (d) spike response of the microring to two pulses of varying interspike interval (ISI), (e) influence of the ISI on the spike response to the second trigger pulse, (f) temporal maps of (d).

To investigate the nonlinear neuron-like dynamics of the microring spiking neuron, we program the arbitrary waveform generator (AWG) to generate a series of electrical patterns. Note that the peak-to-peak AWG output voltage is fixed to 420 mV and directly applied to the microring without any electrical amplification, thus making it possible to scale without TIA for on-chip neuromorphic systems. As shown in Fig. 2(a), the 'negative' output spike first becomes deeper with the increase of electrical perturbation power. Once the perturbation strength crosses the excitability threshold for the last two injected pulses, the microring neuron is triggered to generate constant spikes. Figure 2(b) depicts the dependence of the normalized output on the perturbation strength, and the excitability threshold region is shadowed in gray. Note that the microring neuron belongs to the class II resonate-and-fire neuron without a well-defined threshold[9], thus sub-threshold oscillations can be observed for the first 8 injected pulses. Figure 2(c) is the temporal map plotting the continuous time traces of Fig. 2(a) as cycling patterns. The spike intensity is represented by color, with yellow and blue colors representing spike crests and stable output intensities, respectively. Obviously, similar output patterns are obtained for the 350 incoming stimuli. Hence, the microring neuron can exhibit stable and reproducible spiking responses. Figure 2(d) illustrates the refractory period property, where a single reference pulse is followed by seven pairs of strong perturbation pulses with different interspike intervals (ISIs). For each pulse burst, the first trigger signal can always elicit a complete spike, while the spike

response of the second pulse is partially or fully suppressed. The influence of ISI on the second perturbation pulse is given in Fig. 2(e), where both the relative and absolute refractory period can be clearly observed. Since two complete spikes can be triggered with an ISI of 4 ns, the electrically injected neuron can reach an operation speed of 250 MHz. In this case, the microring neuron also emits stable spiking response over time as shown in Fig. 2(f).

By injecting perturbation pulses with sufficiently high amplitude beyond the excitability threshold and ISIs higher than the refractory period, the microring neuron is able to convert the digital binary signals into spike representations in the optical domain with precise timing. As shown in Fig. 3(a), a bit sequence of '0101010011101101' is successfully encoded into a spike train with high reliability. To demonstrate the temporal integration capacity of the microring neuron, we generate four types of pulse stimuli as given in Fig. 3(b). Following the first reference pulse, a single weak perturbation pulse is designed to only trigger a sub-threshold spike. While the third pulse burst, containing two closely spaced weak pulses with an ISI of 0.25 ns, can trigger a stronger spike generation, and a spike response comparable to the reference spike can be further obtained with a three-spike burst. Finally, we demonstrate controllable inhibitory dynamics of the microring neuron by programming the time interval between an excitatory pattern and an inhibitory pattern. As depicted in Fig. 3(c), the triggered output spikes are gradually suppressed to almost null as the inhibitory patterns move closer to excitatory patterns and recover to their normal shapes as the inhibitory patterns move far away from excitatory patterns. According to the temporal maps in Fig. 3(d-f), reproducible output responses can also be obtained for the above mentioned three cases.

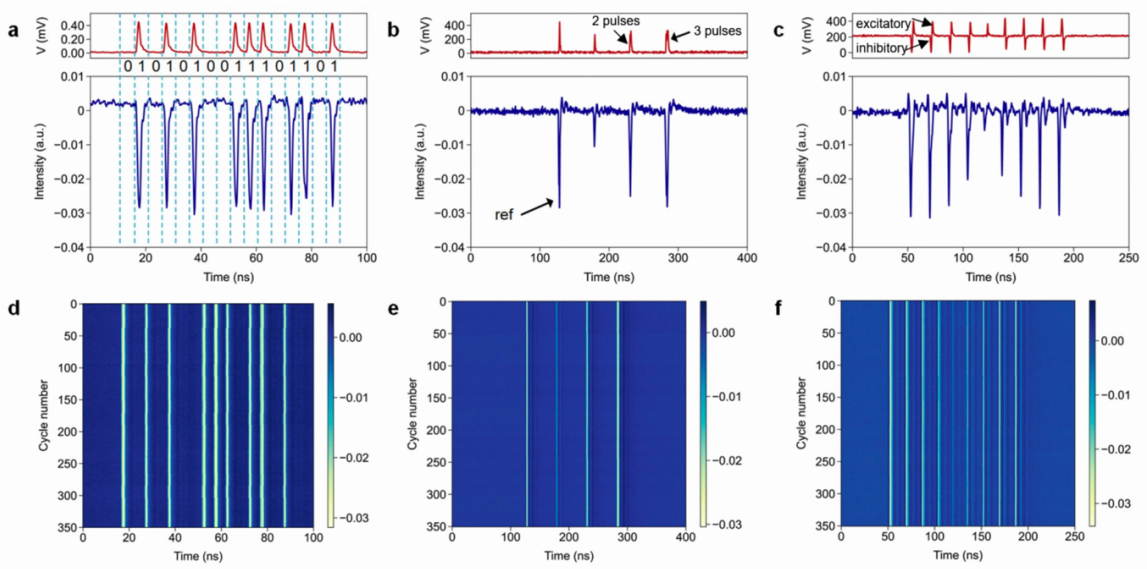


Fig. 3. (a) Binary-to-spike information encoding for return-to-zero input signal at 250 MHz with the electrically injected microring neuron, (b) spiking response of the microring to sub-threshold perturbations, (c) controllable inhibitory dynamics of the microring neuron, (d-f) temporal maps corresponding to (a-c), respectively.

## 3. Conclusion

We have experimentally demonstrated an electrically-injected microring spiking neuron, capable of mimicking key neural dynamics of biological neurons. Besides, its capacity of precise time encoding is verified at a speed of 250 MHz, which is close to the GHz operation speed of laser-based neurons. Combined with on-chip photodetectors, the proposed CMOS-compatible microring neuron makes it promising to build large-scale neuromorphic systems.

## 4. References

[1] B. J. Shastri, "Photonics for artificial intelligence and neuromorphic computing," Nat. Photonics 15, 102-114 (2021).
[2] X. Guo, "Integrated neuromorphic photonics: synapses, neurons, and neural networks," Adv. Photonics Res. 2, 2000212 (2021).
[3] W. Maass, "Networks of spiking neurons: the third generation of neural network models," Neural Netw. 10, 1659-1671 (1997).
[4] P. R. Prucnal, "Recent progress in semiconductor excitable lasers for photonic spike processing," Adv Opt Photonics 8, 228-299 (2016).
[5] J. Robertson, "Ultrafast optical integration and pattern classification for neuromorphic photonics based on spiking VCSEL neurons," Sci. Rep. 10, 1-8 (2020).
[6] B. Ma, "Stochastic photonic spiking neuron for Bayesian inference with unsupervised learning," Opt. Lett. 48, 1411-1414 (2023).
[7] S. Xiang, "Hardware-algorithm collaborative computing with photonic spiking neuron chip based on an integrated Fabry–Perot laser with a saturable absorber," Optica 10, 162-171 (2023).
[8] H. Peng, "Temporal information processing with an integrated laser neuron," IEEE J. Sel. Top. Quantum Electron. 26, 1-9 (2020).
[9] J. Xiang, "All-optical silicon microring spiking neuron," Photon. Res. 10, 939-946 (2022).